ELSEVIER

Determining Cement Composition by Fourier Transform Infrared Spectroscopy

Trevor L. Hughes,* Claire M. Methven,* Timothy G.J. Jones,* Sarah E. Pelham,* Philip Fletcher,† and Christopher Hall*

*Schlumberger Cambridge Research, Cambridge, United Kingdom, and †Schlumberger Dowell Europe-Africa Technology Centre, Aberdeen, United Kingdom

A diffuse reflectance mid-infrared Fourier transform spectroscopy (DRIFTS) method is described for obtaining high quality Fourier transform infrared (FTIR) spectra of cements. DRIFT spectra of synthetic C_3S, C_2S, C_3A, and C_4AF and of pure gypsum, bassanite, anhydrite, syngenite, and calcite are shown. Typical spectra of American Petroleum Institute class G and class A cements display characteristic features which can be related qualitatively to variations in the constituent minerals. For quantitative analysis, the FTIR spectra of 156 cements of varied origin and known elemental composition have been used to construct multivariate calibration models. These relate the spectrum to composition (expressed in terms of nine mineral components and five minor oxides) and allow the composition of unknown cements to be determined rapidly from the FTIR spectrum alone. Error estimates are given. ADVANCED CEMENT BASED MATERIALS 1995, 2, 91–104

KEY WORDS: Analysis, Diffuse reflectance mid-infrared Fourier transform spectroscopy, Fourier transform infrared spectroscopy, Mineralogy, Oilwell cement, Portland cement

Cements are variable and sometimes unpredictable in their hydration behavior. In oilfield cementing, variability is an everyday practical problem which imposes a heavy burden of performance testing on those who routinely design complex slurries with many additives. From time to time, the unpredictability of cements leads to serious operational failures. Rapid and accurate characterization methods are therefore urgently needed to screen oilwell cements (for example, in a user's quality control laboratory) and to identify cements that may produce abnormal slurry performance. Here we describe a new method based on Fourier transform infrared (FTIR) spectroscopy for the rapid determination of cement composition. This method identifies clinker and accessory minerals which influence cement performance. The work is part of a wider study of FTIR methods in cement chemistry which extends also to the direct prediction of performance properties from FTIR spectra [1] and the in-situ monitoring of hydration reactions [2]. This in turn can be seen as part of the current rapid evolution of FTIR spectroscopy in the analysis of complex materials [3–5].

Recently Uchikawa [6] has reviewed advances in methods of physicochemical characterization of clinkers, cement powders, hydrated cements, and concrete. Simpson [7] has surveyed analytical methods for cement in relation to oilfield engineering. Methods of determining cement composition fall into two groups: (1) those (like atomic absorption spectroscopy (AAS) [8], inductively coupled plasma emission spectrometry (ICP) [9], and X-ray fluorescence spectrometry (XRF) [8], as well as traditional wet chemical methods [10]) which provide an elemental analysis of the bulk composition (usually expressed formally in terms of equivalent oxides); and (2) those (like X-ray diffraction [11], optical [12] and electron microscopy [13], and thermogravimetric analysis (TGA) [14,15]) which determine constituent minerals more or less directly. The FTIR method used here belongs essentially to the second group in that the infrared absorption spectrum is a property of the mineral lattice. However, for quantitative analysis we choose to relate the infrared spectrum to the composition by means of chemometric models which we calibrate by reference to accurate elemental analysis. In that sense, the method as described here is somewhat hybrid. However, alternative calibration schemes are possible. We discuss this further below.

Infrared spectroscopy has not been much used in the quantitative analysis of cement materials. The main uses have rather been in identification of minerals [16–22] and in structural studies [23,24]. Most published cement infrared spectra [20,24] have been collected by transmission methods. Here, however, we use diffuse reflectance mid-infrared Fourier transform spectroscopy (DRIFTS) for both qualitative and quantitative

Address correspondence to: Trevor L. Hughes, Schlumberger Cambridge Research, High Cross, Madingley Road, Cambridge, CB3 OEL, United Kingdom.
Received March 3, 1994; Accepted June 20, 1994

ISSN 1065-7355/95/$9.50
SSDI 1065-7355(94)00031-8

Advn Cem Bas Mat
1995;2:91–104

analysis. DRIFTS has marked advantages over transmission methods in spectrum quality and speed. A carefully acquired DRIFT spectrum provides an objective signature of the cement sample which is largely determined by the mineralogical composition and texture of the material and which is rich in information. The DRIFTS signature can be used qualitatively but can also be interpreted quantitatively in terms of composition by using multivariate calibration models and nontraditional statistical methods of several kinds.

Experimental

Materials

Potassium bromide (FTIR grade), gypsum $CaSO_4 \cdot 2H_2O$, bassanite $CaSO_4 \cdot \frac{1}{2}H_2O$, and anhydrite $CaSO_4$ (ACS reagent grade) were supplied by Aldrich Chemical Co. (Gillingham, UK). A natural sample of syngenite $K_2Ca(SO_4)_2 \cdot H_2O$ was donated by the British Museum (London, UK). The mixture of calcium hydroxide and calcium carbonate was prepared by aging a sample of calcium hydroxide (Koch-Light) in air. The pure phases C_3S, C_2S, C_3A, and C_4AF (C = CaO, S = SiO_2, A = Al_2O_3, F = Fe_2O_3) were prepared and supplied by Construction Technology Laboratories (Skokie, Illinois). Standard reference cements were obtained from NIST (Standard Reference Materials program). Commercial cements were obtained worldwide from a variety of industry sources.

Chemical Analysis and Other Support Measurements

Elemental analyses (Na, Mg, Al, Si, P, K, Ca, Ti, Cr, Mn, Fe, Zn, Sr) were carried out by standard ICP methods. Loss on ignition, free lime, and insoluble residue determinations were by ASTM methods [10]. Blaine fineness was measured by an improved method yielding ±1% precision [Hughes and Methven, unpublished]. Particle-size distributions were determined by a light-scattering method using a CILAS instrument. Bogue compositions were calculated according to the American Petroleum Institute (API) procedure [25]. This differs somewhat from the Bogue calculation commonly used in the cement industry (for example, in omitting the free lime adjustment).

DRIFTS Technique

Fuller and Griffiths [26,27] first showed that it was possible to measure DRIFT spectra rapidly and with a high signal:noise ratio. This led to the introduction of commercial DRIFTS accessories. Infrared radiation from a Michelson interferometer is focused onto the sample surface via an ellipsoidal mirror (Figure 1). Radiation impinging on the sample experiences a combination of specular (surface) reflection and diffuse reflection in which incident radiation penetrates into the bulk of the sample and undergoes multiple scattering and absorption before reemerging with a wide angular

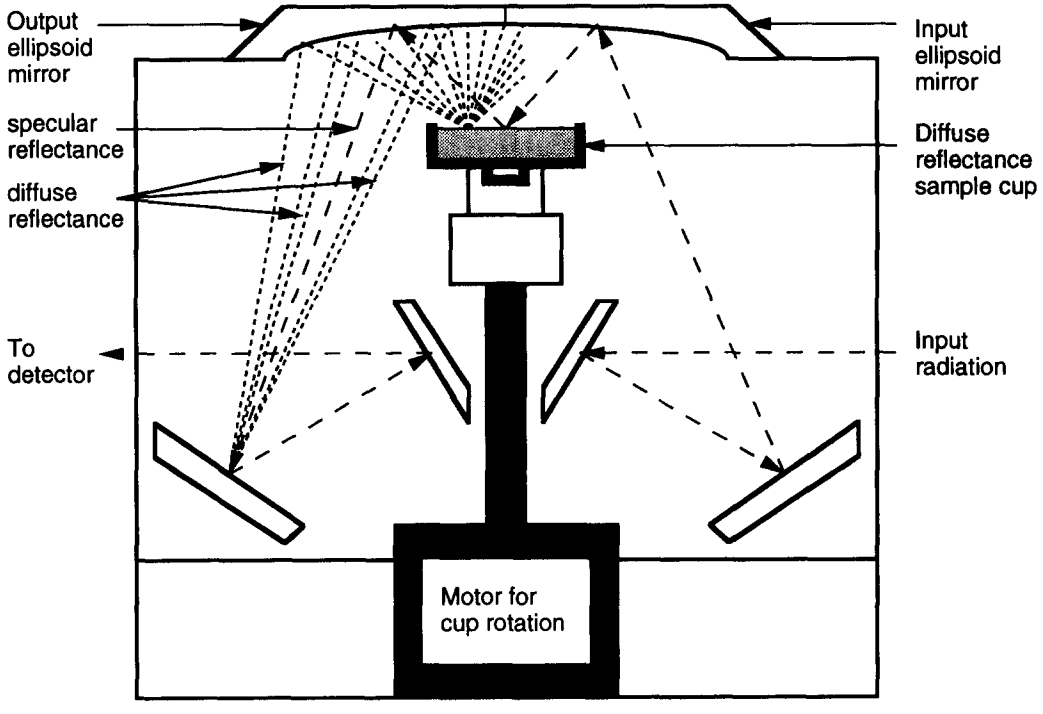

FIGURE 1. Schematic of DRIFTS accessory.

distribution. The reflected radiation is collected by a second ellipsoidal mirror.

The DRIFT spectrum of the substance of interest is normally measured using a nonabsorbing material as a comparison: finely divided alkali halides (e.g., KBr) are commonly used in the mid-infrared region (4000 to 400 cm^{-1}). We denote by R_∞ the diffuse reflectance, the ratio of the diffuse radiant power reflected from the sample to that from the comparison or reference material. The subscript denotes that the sample is thick (semiinfinite) compared with the penetration depth of the diffusely scattered radiation. The absorbance $A = -\log R_\infty$; all spectra shown here are in the form $A(\tilde{\nu})$, absorbance against wavenumber.

Equipment, Procedures, and Repeatability

Spectra were recorded on a Nicolet 5DX FTIR spectrometer equipped with a DTGS detector and a Spectra-Tech Collector™ diffuse reflectance accessory, modified to allow steady rotation of the sample during scanning. Spectra were acquired at 4 cm^{-1} resolution. Essential ancillary equipment included (1) a tungsten carbide ball mill (Retsch MM2 type) to grind KBr to a repeatable particle-size distribution; (2) a purpose-built compaction device to achieve a controlled packing density of sample and reference materials in matched cups; and (3) a source of dry, CO_2-free air to purge spectrometer optics and sample compartment.

Our procedure for the acquisition of a high quality DRIFT spectrum involves the following steps. (1) KBr (5.0 g) is ground for 5 minutes at a standard speed; fresh KBr is prepared daily. (2) Ground KBr (0.4500 g) is compacted into a sample cup and the surface leveled flush with the rim. (3) The sample compartment is purged and a multiscan DRIFT reference spectrum is acquired. (4) A cement sample (0.0450 g) is dispersed in 0.4050 g KBr by gentle mixing and steps 2 and 3 are repeated. The cement spectrum is obtained as the ratio of the mixture spectrum to the reference spectrum. Sample preparation and spectrum acquisition take only about 15 minutes. For quantitative work, it is critical to acquire high quality spectra in a consistent and repeatable way and for this it is essential to follow a closely defined experimental procedure.

The relation between the DRIFTS reflectance R_∞ and the concentration of absorbing components is described approximately by the Kubelka-Munk equation [28]:

$$R_\infty = \{1 - [K/(K + 2S)]^{1/2}\}/\{1 + [K/(K + 2S)]^{1/2}\}. \quad (1)$$

K and S are absorption and scattering coefficients, and for dilute absorbers $K = \Sigma a_i c_i$, where a_i is the absorptivity (for example, as calculated conventionally in transmission spectroscopy from the Beer-Lambert law), and c_i is the concentration of component i. Since the mineralogy of the sample is largely associated with the absorptivity, it is clearly important to keep variation in the scattering coefficient to a minimum. Furthermore, the Kubelka-Munk equation shows that $1 - R_\infty$ varies approximately as $c^{1/2}$ for dilute absorbers. Therefore, in optimizing the concentration of cement in the KBr matrix, we need to find a balance between several effects.

We wish to maximize the signal:noise ratio and minimize sample weighing error without introducing an unacceptable contribution to the scattering from the cement sample. Higher concentrations improve the counting statistics since the spectroscopic signature is averaged over a larger number of cement particles, reducing the error in estimating the bulk composition from the sample composition. Our standard procedure employs 10 weight percent (wt%) of cement dispersed in ground KBr. Figure 2 shows the effect on the spectroscopic data of varying the cement concentration in the mixture. The region 1100 to 500 cm^{-1}, which includes most of the bands from the clinker minerals, is increasingly distorted as the cement concentration increases. Figure 3 confirms that absorbance varies nonlinearly with cement concentration and that repeatability is optimal when the cement concentration is $\leq$10 wt%. Other workers [29,30] applying DRIFTS methods to the analysis of other materials have used higher dilutions to reduce scattering.

The particle-size distribution of the KBr and its compaction are tightly controlled to ensure that the radiation penetrates into the matrix to a repeatable depth. It is important that the interaction volume should be constant. Figure 4 shows how spectroscopic data change as the KBr particle size is altered. Unground KBr (spectroscopic grade as received) allows incident radiation to penetrate deeply, resulting in a high sample absorbance. Reducing the particle size by grinding reduces the penetration depth, and by increasing S in the Kubelka-Munk equation causes the absorbance to decrease. In our experience, spectrum repeatability is optimal when KBr is ground for 5 minutes: unground KBr is difficult to compact and level, and prolonged grinding produces an increasingly hygroscopic powder.

Typical duplicate DRIFT spectra of two oilfield cements, API class G and API class A, are shown in Figure 5. Differences between duplicate spectra are less than 0.01 absorbance unit across the entire spectrum; it can be seen that these differences are small compared with the differences between the mean spectra of the two cements. The procedure which we describe ensures that the spectroscopic variance for different cements is dominated by the variance in mineralogical composition, although there is some contribution due to variance in cement particle-size distribution [1].

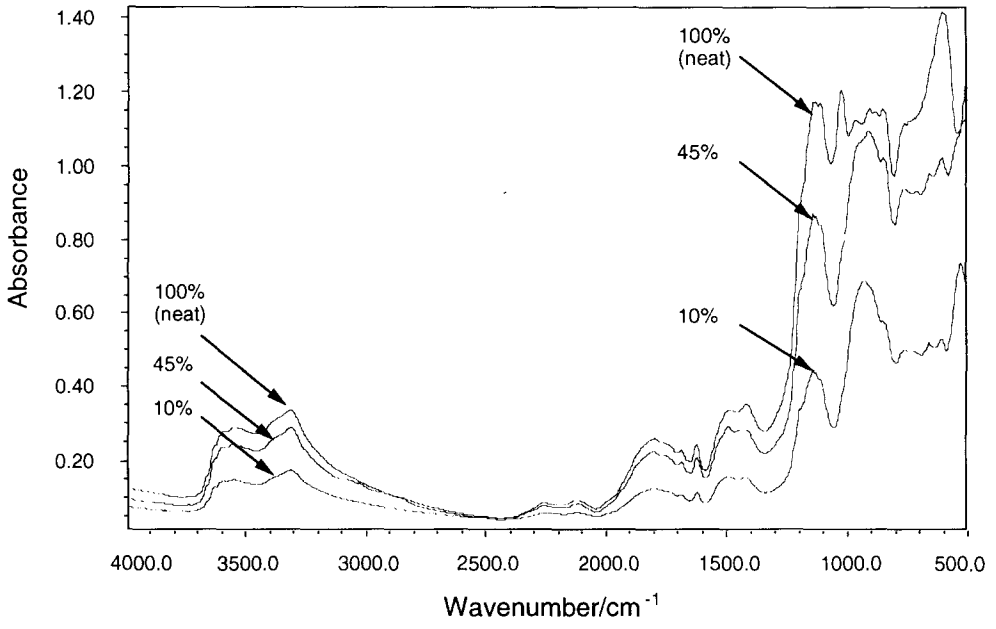

FIGURE 2. Effect of varying cement concentration dispersed in the KBr matrix.

Multivariate calibration for quantitative analysis was carried out using chemometric software written within the laboratory.

Spectra of Cements and Cement Minerals

Spectra of Pure Minerals

In Figure 6 we show the DRIFT spectra of pure samples of the main cement minerals. An assignment of the absorption bands is given in Table 1.

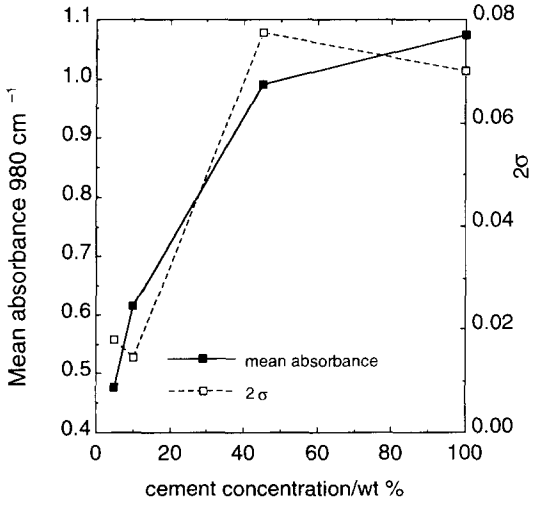

FIGURE 3. Effect of varying cement concentration on absorbance and repeatability, measured at 911 cm^{-1}; 2σ is the standard deviation of repeat measurements (n = 3).

The major absorption bands of the clinker phases are in the region 2100 to 500 cm^{-1}. The Si-O stretching mode produces an absorption band at 935 cm^{-1} in C_3S, while a broader band with peaks at 991, 879, and 847 cm^{-1} is observed in C_2S. Overtones in the region 2060 to 1600 are also characteristic of silicates. The C_3A spectrum shows a broad Al-O stretching band in the region 900 to 760 cm^{-1}. This is very different from the C_4AF spectrum, which shows a broad, poorly resolved band in the region 750 to 500 cm^{-1}.

The hydrated minerals have distinctive signatures due to O-H stretching and bending vibrations; in addition, the ν_3 fundamentals and overtones are particularly useful in distinguishing between the various sulfate minerals. The spectrum of the mixture (Figure 6b) shows distinct features due to each component: the hydroxides of calcium and magnesium have distinct O-H stretching frequencies and calcium carbonate has characteristic fundamentals and overtones well separated from the sulfate bands. The polymorphs of calcium carbonate can be distinguished by differences in the ν_3 carbonate band in the region 1550 to 1350 cm^{-1}.

These characteristic features can be used as simple diagnostics and allow abnormalities in composition to be detected readily.

Qualitative Interpretation of Cement Spectra

The pure component spectra shown in Figure 6 provide a basis for a qualitative interpretation of cement spectra. For example, the class G cement shown in Figure 5a is evidently one in which gypsum and syngenite are the dominant sulfate minerals. It is also clear

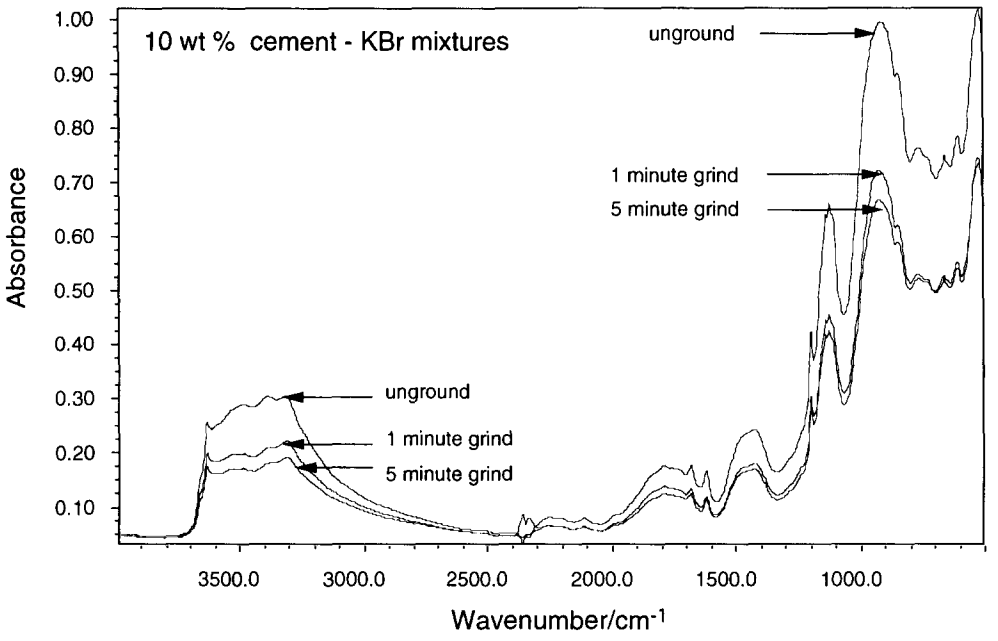

FIGURE 4. Effect of varying the particle size of the KBr matrix.

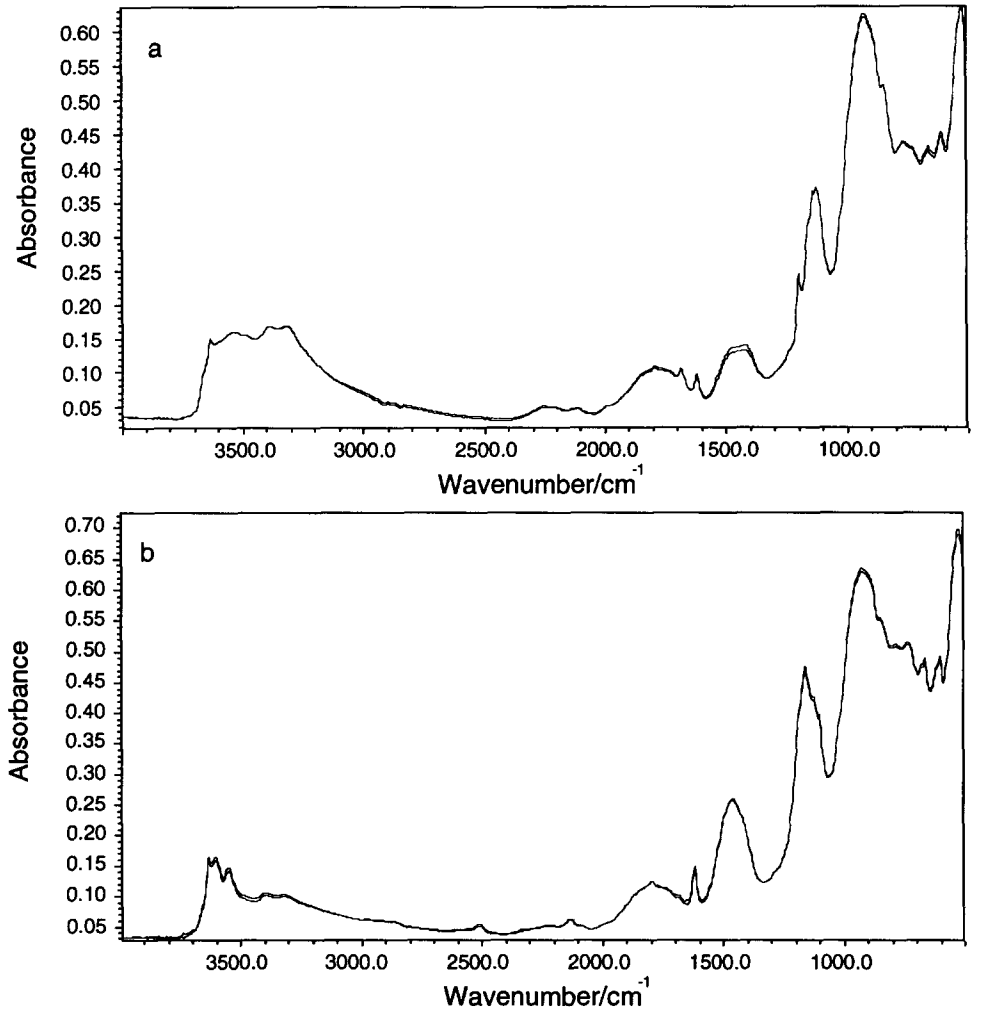

FIGURE 5. Duplicate DRIFT spectra of example cements: (a) API class G; (b) API class A.

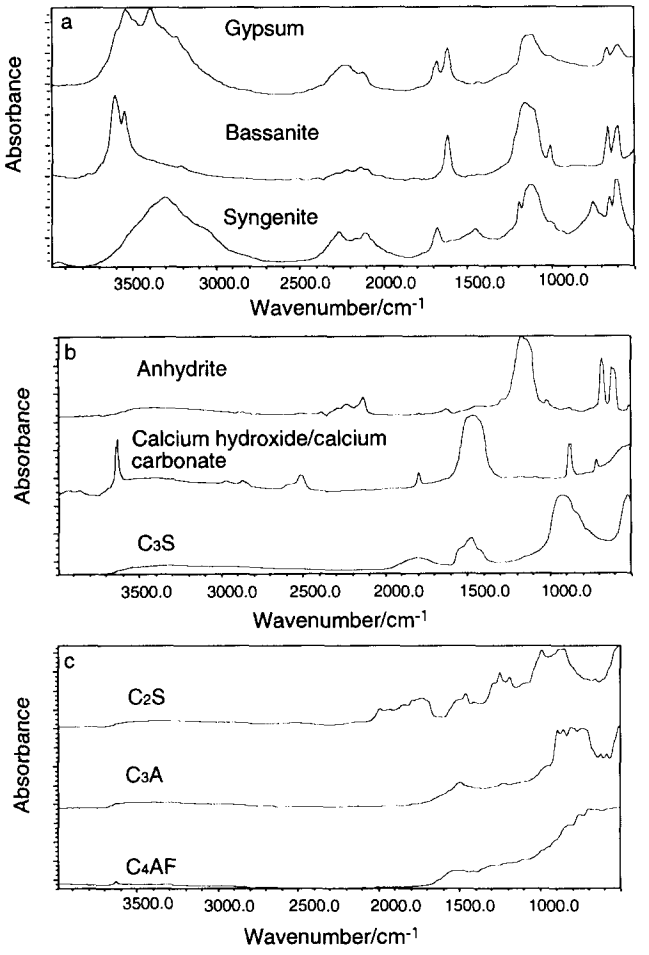

FIGURE 6. DRIFT spectra of pure components: (a) gypsum, bassanite, and syngenite; (b) anhydrite, calcium hydroxide/calcium carbonate, and C_3S; (c) C_2S, C_3A, and C_4AF.

that appreciable quantities of both calcium hydroxide and calcium carbonate are present. Spectroscopic features in the region 900 to 600 cm^{-1} show that this cement has a low C_3A:C_4AF ratio. In contrast, the spectrum shown in Figure 5b reveals a bassanitic cement that contains high concentrations of calcium hydroxide and carbonate and has a higher C_3A:C_4AF ratio.

Comparison of Transmission and DRIFTS Spectra

Figure 7 compares the transmission and DRIFT spectra of a class G cement. The transmission spectrum was obtained using a conventional KBr pressed disk containing 0.0010 g sample and 0.2500 g KBr. The penetration depth in the DRIFTS experiment is about 200 μm, approximately 10% of the total bed depth. Consequently, the DRIFT spectrum is averaged over a larger, and therefore more representative, mass of cement. The DRIFT spectrum also exhibits enhanced absorption bands due to interstitial phases (800 to 850 cm^{-1}), sulfate minerals (3620 to 3200, 1600 to 1580, and 1300 to 1060 cm^{-1}), calcium carbonate (1580 to 1320 cm^{-1}), and calcium hydroxide (3645 cm^{-1}). Figure 8 compares the transmission and DRIFT spectrum of pure calcium carbonate; in the DRIFT spectrum, overtone absorptions (3050 to 2750, 2680 to 2380, 2260 to 2080, 1950, and 1794 cm^{-1}) are more prominent than in transmission. The enhancement of overtone and combination bands (relative to fundamentals) is common in DRIFT spectra and provides a valuable advantage in spectral variance.

Quantitative Analysis of Cements

Multivariate Approach

The simple application of the Beer-Lambert law (or its Kubelka-Munk equivalent for diffuse reflectance) is impossible for complex multicomponent mixtures with many broad and overlapping absorption bands. However, a number of multivariate statistical techniques [31–33] have been successfully applied to many such systems, by means of which calibration models can be constructed without prior knowledge of the origin of the absorption bands. These techniques allow a regression model to be established between a matrix **A** of absorbances at p wave numbers for m samples and a matrix **C** of composition data. **C** contains, for example, concentration data for n components in the same m samples. For cement analysis, we use a partial least squares (PLS) method [32]. In essence, the absorbance matrix **A** and the composition matrix **C** are reduced to smaller matrices of spectral and composition factors between which a regression relationship is then found.

Calibration Methods

A common approach to the calibration of a multivariate model is to prepare a set of mixtures of pure components and to use these as calibration standards. This approach is difficult if not impossible for DRIFTS analysis of cements for at least two reasons. First, the clinker minerals vary in composition from cement to cement and synthetic clinker phases of ideal composition do not provide satisfactory single-component spectra for commercial cements. Second, the spectrum is sensitive to the particle-size distribution of the sample. Therefore, multicomponent calibration mixtures of pure minerals must not only span the variance of the clinker phase mineralogy but must also reflect the complex relation between mineralogy and particle-size distribution of production cements. To prepare such a calibration set (including subsets of synthetic alites, belites, and interstitial minerals with representative substitution ions and of varying particle-size distribu-

TABLE 1. Characteristic absorbance bands for cement minerals

Mineral	Fundamentals			Overtones	O-H Stretch	O-H Bend
Sulfates	ν_1	ν_3	ν_4			
Gypsum	1005	1117	669, 604	2500–1900	3553, 3399	1686, 1618
Bassanite	1009	1152, 1117, 1098	660, 629, 600	2500–1900	3611, 3557	1618
Syngenite	1001	1192, 1130, 1113	658, 644, 604	2500–1900	3309	1678
Anhydrite	1015	1163	677, 615, 600	2500–1900		
Carbonates Hydroxides	ν_2	ν_3	ν_4			
Calcium Carbonate	876, 849	1458	714	2980–2500, 1794		
Calcium Hydroxide					3646	
Magnesium Hydroxide					3696	
Clinker phases		Unassigned Fundamentals				
C_3S	Si–O	935, 521		2000–1600		
C_2S	Si–O	991, 879, 847, 509		2060–1600		
C_3A	Al–O	889, 860, 812, 785, 762, 621, 586, 518, 506				
C_4AF	Fe–O	700–500				

tion) is a large undertaking. We note in passing that the original particle-size distribution of the cement is preserved in the DRIFTS method described here.

We have chosen an alternative approach in which we build a calibration model directly from measurements on a large set of cements, chosen to have representative variance in composition and particle-size distribution. For the calibration model described here, we used a total of 156 calibration cements, gathered from a variety of cement suppliers and oilfield locations throughout the world. To maximize the variance,

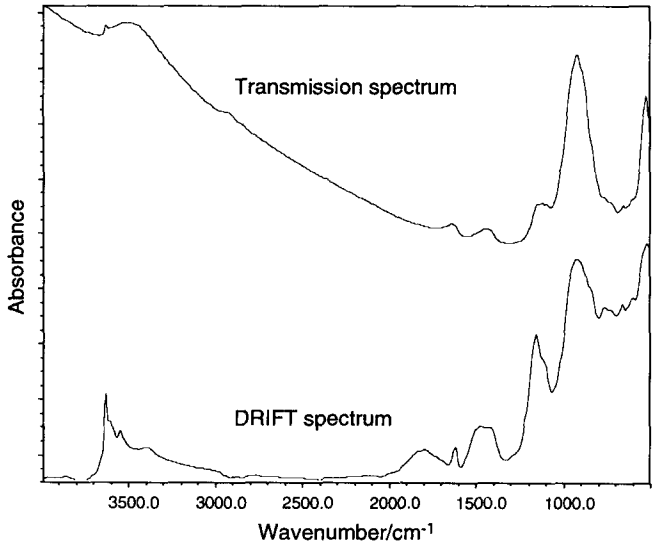

FIGURE 7. Transmission and DRIFT spectra of an example class G cement.

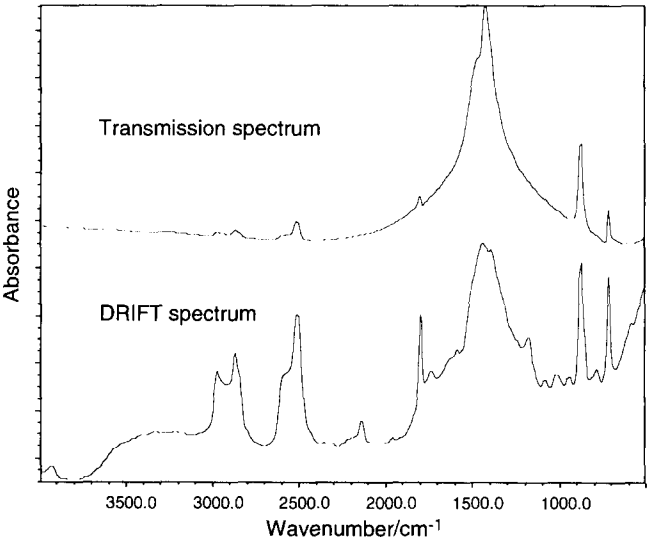

FIGURE 8. Transmission and DRIFT spectra of calcite.

Advn Cem Bas Mat
1995;2:91–104

API class G, class H, and class A cements are included. The calibration set was designed to be representative of cements that are commonly encountered in oilfield engineering; thus, it includes aged as well as recently manufactured materials. Class A cements are essentially type 1 construction cements, so that the calibration model described here in fact encompasses a large fraction of the Portland cements manufactured worldwide. The spectrum of each calibration cement, together with duplicate spectra for more than half of the samples, is included in the matrix **A**, which contains a total of 236 DRIFT spectra.

For these calibration cements, we do not, of course, know the mineralogy by direct independent methods. While mineralogical analysis of each of these 156 cements could have been attempted, the accuracy of mineralogical assays of cement powders is quite poor. Instead, we have used bulk chemical analysis, which today provides by far the most accurate compositional data on cement materials, as the independent basis of our calibration. Instrumental chemical analysis, expressed as equivalent oxide composition, supplemented by data on free lime, ignition loss, and acid-insoluble residue can be transformed in several ways to yield estimates of the mineralogical composition of the cement. The simplest of these element-mineral transforms is the Bogue calculation. Here we use the API variant [25]. There are numerous modified or "improved" Bogue calculation methods, of which the most elaborate is that of Taylor [34]. We regard the API Bogue calculation of the clinker phase assemblage first and foremost as a simple linear transformation of the C, S, A, and F oxide data. In determining the API Bogue composition from the DRIFT spectrum, we emphasize that we are determining the API Bogue composition *which would be calculated from oxide data if known*, not the true mineralogy of the cement. This, of course, is exactly what is required for some quality control purposes (for example, in oilfield cementing [25]). It should be noted that calibration models can equally well be constructed on the basis of other representations of the oxide data or indeed on the oxide data themselves.

The concentration of the various sulfate minerals in each calibration cement is calculated by assuming that the total SO_3 is partitioned between the four sulfate minerals gypsum, bassanite, anhydrite, and syngenite. (No attempt has been made here to allow for SO_3 substituted in the clinker phases.) The quantities of each mineral are then determined directly from the DRIFTS spectrum for each calibration cement. The spectra of simple mixtures of gypsum, bassanite, syngenite, and anhydrite have been used to establish regression equations based on ratios of particular spectral features. This approach is justified on the grounds that the sulfate minerals are present in cements in relatively pure forms, mostly mechanically admixed with the clinker phases. The amount of syngenite present should always be less than 3.487 (K_2O).

Figure 9 shows that the peak area of the O-H stretching band at 3646 cm^{-1} is proportional to the calcium hydroxide concentration as measured by TGA for a subset of the cements. This relationship is used to determine the TGA equivalent calcium hydroxide concentrations in each calibration cement. A similar approach is used to determine the calcium carbonate concentration (Figure 9b).

In all, we express the composition of each cement in terms of nine mineral components: API Bogue C_3S, C_2S, C_3A, and C_4AF; gypsum and bassanite; syngenite; and calcium hydroxide and calcium carbonate. Composition data for each calibration cement form the matrix **C**. This nine-mineral model includes the main clinker components as well as components that are

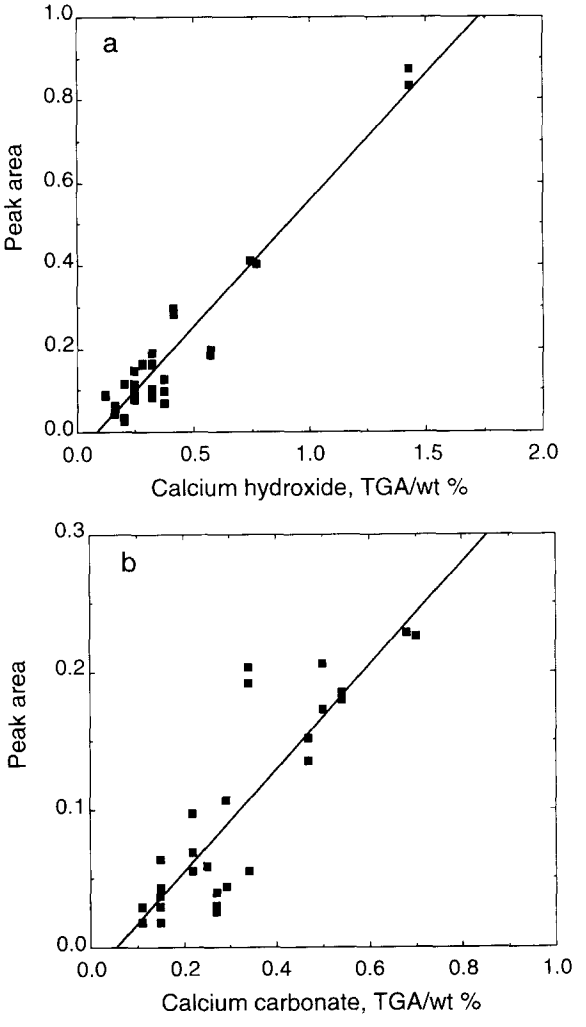

FIGURE 9. Relationships between peak area and TGA analyses for (a) calcium hydroxide (band at 3646 cm^{-1}) and (b) calcium carbonate (overtone at 2650 to 2450 cm^{-1}).

diagnostic of the chemistry of the sulfate subsystem and of changes occurring in cements during aging.

Spectroscopic Data Reduction and PLS Models

Each DRIFT spectrum at 4 cm^{-1} resolution is a data record comprising some 900 numbers. All are reduced in size to make the calibration database more manageable before the PLS model is computed. Data reduction is achieved by (1) excluding the region 2390 to 2290 cm^{-1} sensitive to atmospheric carbon dioxide; (2) reducing resolution to 8 cm^{-1}; and (3) eliminating baseline shifts by using a multiplicative scattering correction [35]. After data reduction, **A** is a 236 × 411 matrix. **A** and **C** are divided into a calibration set ($\mathbf{A}_c$ and $\mathbf{C}_c$; 142 data records); a validation set ($\mathbf{A}_v$ and $\mathbf{C}_v$; 71 data records); and an independent test set ($\mathbf{A}_i$ and $\mathbf{C}_i$; 23 data records). The calibration matrix includes 80 data records corresponding to "extreme" cements which have outer range values of one or more component concentrations. Apart from this special allocation of extreme samples, dividing the matrix is a random process. However, pairs of data records corresponding to duplicate spectra are always kept together. The PLS model itself is constructed by using the calibration matrices $\mathbf{A}_c$ and $\mathbf{C}_c$ to generate PLS matrices; the validation matrices $\mathbf{A}_v$ and $\mathbf{C}_v$ are then used to choose the optimum number of factors for each analyte. Matrices $\mathbf{A}_i$ and $\mathbf{C}_i$ are not used in computing the model, but provide a test data set for evaluating the precision and accuracy of the model. In the following discussion, we refer to two PLS models for cement analysis: M1, a nine-mineral model for C_3S, C_2S, C_3A, and C_4AF; gypsum and bassanite; syngenite; and calcium hydroxide and calcium carbonate; and M2, a supplementary

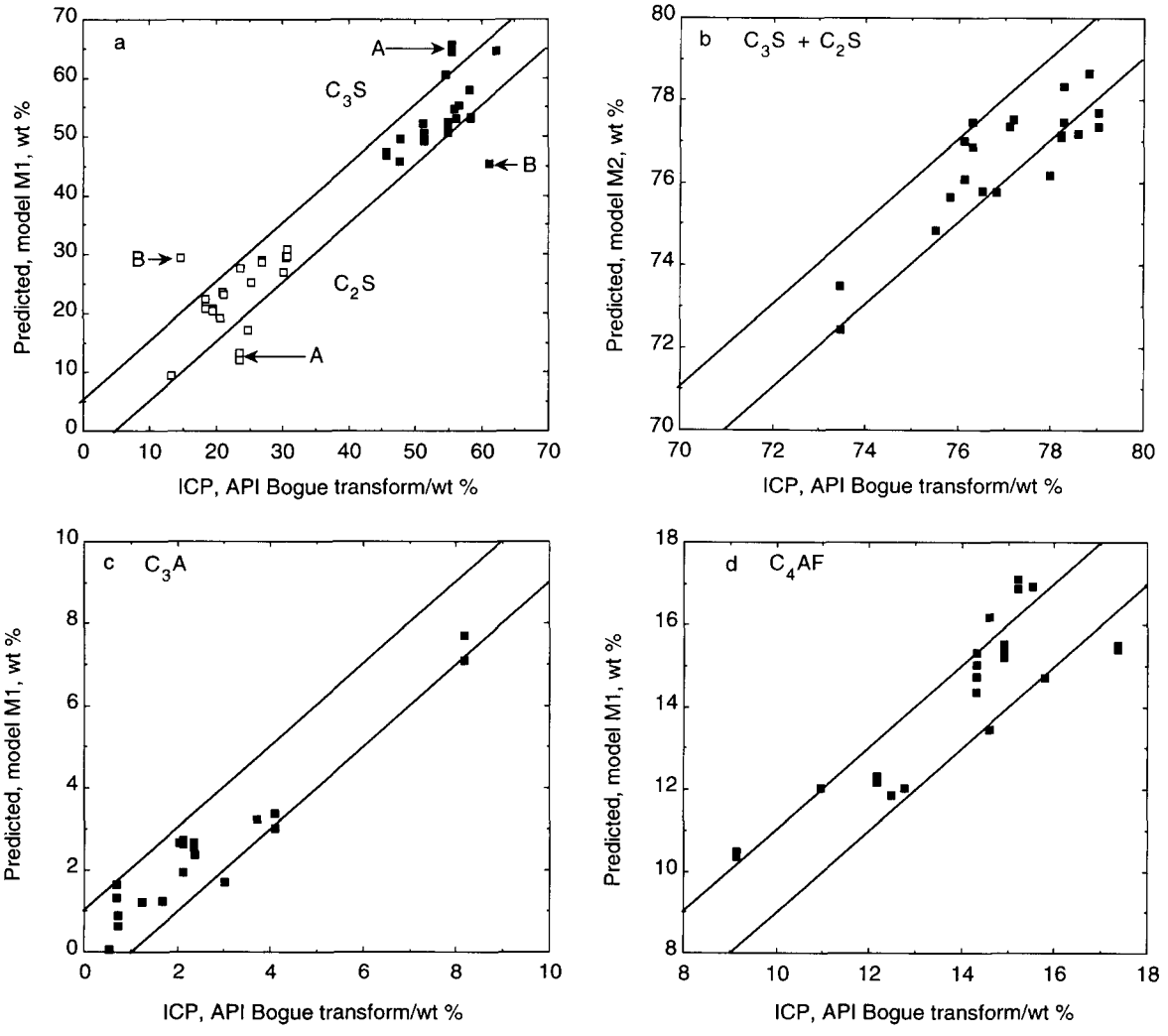

FIGURE 10. Predicted concentrations of the clinker phases versus measured values given by an API Bogue transform of the ICP oxides data: (a) C_3S and C_2S; (b) C_3S + C_2S; (c) C_3A; (d) C_4AF. The 45° lines define limits for least accurate determinations (excluding outliers).

model that determines C_3S + C_2S, SO_3, Na_2O, K_2O, P_2O_5, and MgO.

Cements

Figures 10 to 12 compare the predicted and measured component concentrations for the independent test set which includes duplicates for seven cements. The statistical diagnostics for M1 and M2 and values of precision and accuracy for the independent test set are given in Table 2.

We see that the C_3S and C_2S concentrations determined using M1 are within ±5 wt% of the values calculated from oxide data. To put these errors in perspective, we need to estimate the probable errors in the calculated API Bogue (measured) values against which the DRIFTS predictions are tested. The errors in these calculated values arise from analytical error in the chemical analysis. To this must also be added a sampling error, since the sample used for DRIFTS and that used for chemical analysis are not identical, although both are taken from the same batch.

The analytical errors, although small in themselves, lead to relatively large uncertainties in the C_3S and C_2S because of the nature of the Bogue function. From typical analytical errors, we estimate the errors in calculated C_3S and C_2S individually to be around ±2.8 wt%. Thus, a large part of the DRIFTS prediction errors can be attributed to uncertainties in the calculated values. However, as is well known (and suggested in Figure 10a for outlier cements A and B, which are not outliers in Figure 10b), there is a strong inverse correlation between C_3S and C_2S, and the error in the sum (C_3S + C_2S) due to analytical errors is much smaller (±0.6 wt%). This is true also of the prediction from the DRIFTS model M2. The accuracy of the (C_3S + C_2S) estimate is ±1.8 wt% (compared with an analytical error of ±0.6 wt%).

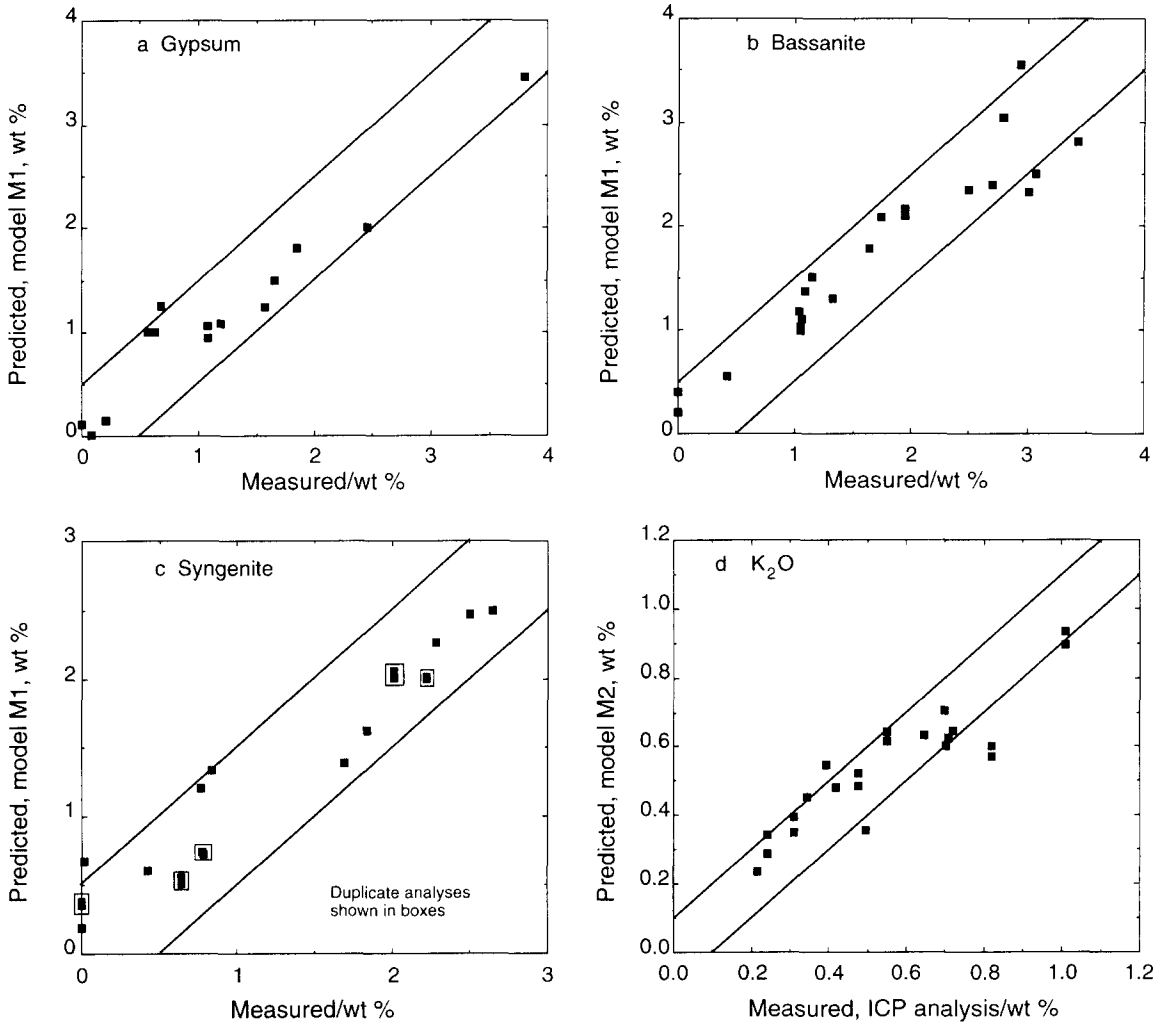

FIGURE 11. Predicted concentrations of (a) gypsum, (b) bassanite, (c) syngenite, and (d) K_2O versus measured values calculated from spectral data and by ICP analysis (see text).

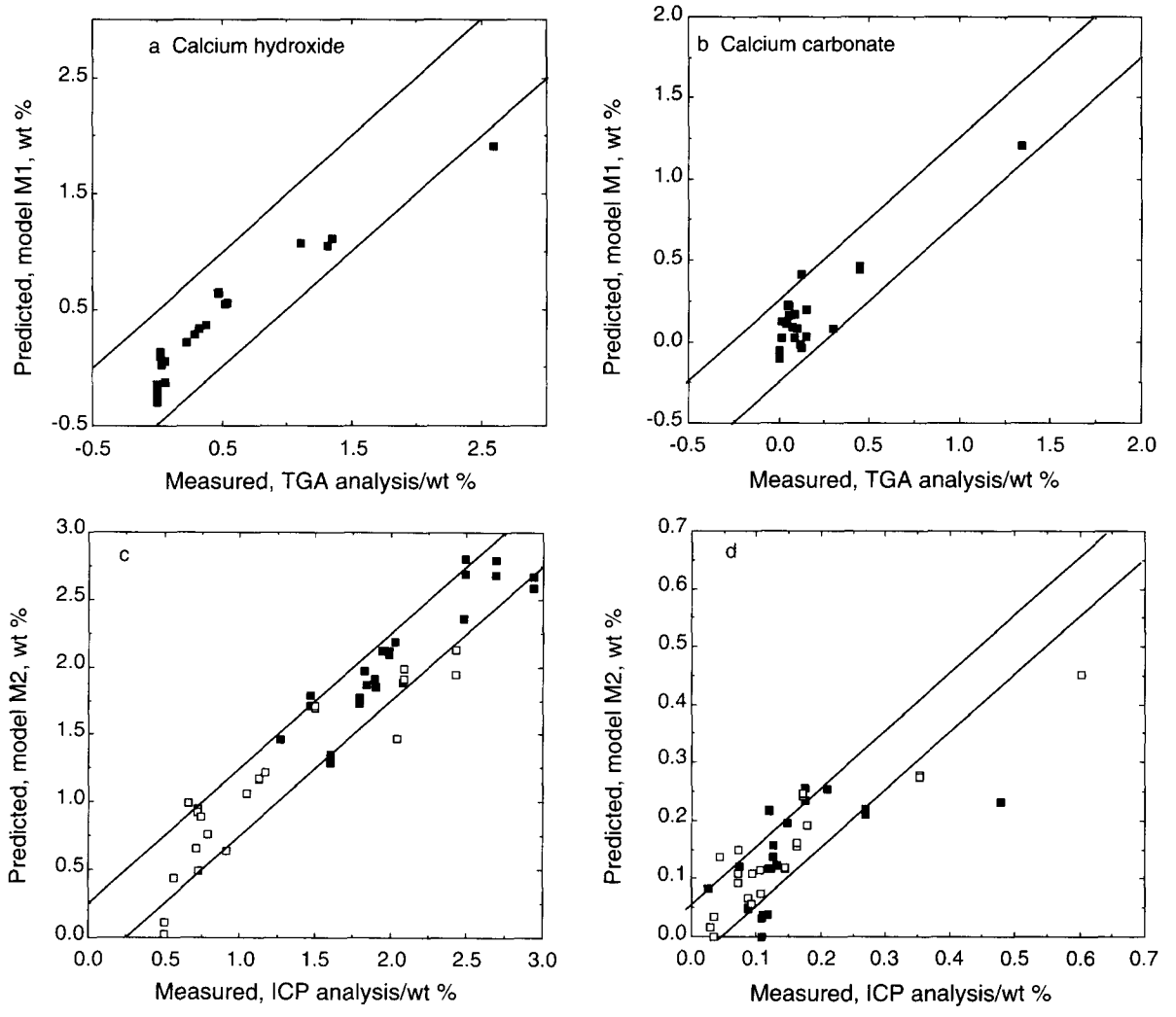

FIGURE 12. Predicted concentrations of (a) calcium hydroxide, (b) calcium carbonate, (c) SO_3 (■) and MgO (□), and (d) Na_2O) (■) and P_2O_5 (□) versus measured values by TGA and ICP analysis.

The predicted C_3A and C_4AF are accurate to within ±1.5 and ±2.0 wt%, respectively. These errors compare with ±0.2 and ±0.6 wt% errors arising directly from analytical errors in the bulk chemical analysis.

The prediction of the nonclinker minerals by M1 is generally good. This is a particular strength of the method and arises at least in part from the concentration of these minerals in the finer fractions of the particle-size distribution, thus given these components relatively large weightings in the DRIFT spectrum. A general trend in the results is that precision is higher than accuracy, and this is especially evident for analyses of the sulfates, for example, syngenite (Figure 11c).

Results of predictions using M2 show that the DRIFT spectra also embody features that allow us to determine several of the minor oxides, including MgO and the alkalis. Figure 11c and d shows that we can separately estimate syngenite (one of several K-containing minerals) and total K_2O. Figure 12 shows that analyses of SO_3, MgO, Na_2O, and P_2O_5 are accurate to within about ±0.3, ±0.5, ±0.1, and ±0.1 wt%, respectively. Mg, Na, and P are mainly present as substituents in clinker phases and their determination via M2 presumably arises through small perturbations of the clinker phase absorption bands.

Certified Reference Cements

In Table 3 we show the results of applying the DRIFTS method to the analysis of four standard reference cements. Here we have used the certified chemical analysis to calculate API Bogue clinker phase compositions. The sulfate, hydroxide, and carbonate minerals are estimated from individual spectra according to the method described. The M1 and M2 model predictions are generally in good agreement with the independent estimates and provide further validation of the DRIFTS methodology. However, the results highlight inaccuracies that can occur if analysis involves extrapolation

TABLE 2. Model diagnostics: precision and accuracy for test data

Component	Number of Factors[a]	Linear Correlation Coefficients			Precision wt %[b]	Accuracy	
		Calibration	Validation	Test		RMSE wt %[c]	Within ±wt %[d]
M1							
C_3S	13	0.765	0.755	0.559	0.56	2.90[e]	5.0[e]
C_2S	15	0.828	0.798	0.570	0.63	3.10[e]	5.0[e]
C_3A	16	0.983	0.954	0.954	0.67	0.31	1.5
C_4AF	17	0.977	0.959	0.868	1.08	0.18	2.0
Gypsum	16	0.919	0.858	0.977	0.33	0.11	0.6
Bassanite	24	0.959	0.925	0.945	0.33	0.07	0.6
Syngenite	25	0.944	0.918	0.953	0.29	0.04	0.5
$Ca(OH)_2$	20	0.972	0.927	0.957	0.19	0.02	0.3
$CaCO_3$	39	0.995	0.940	0.901	0.12	0.05	0.3
M2							
$C_3S + C_2S$	26	0.899	0.828	0.862	0.91	0.55	1.8
SO_3	27	0.968	0.956	0.911	0.18	0.07	0.3
Na_2O	30	0.928	0.755	0.577	0.08	0.01	0.1
K_2O	36	0.977	0.903	0.906	0.10	0.03	0.2
MgO	20	0.841	0.806	0.914	0.26	0.06	0.5
P_2O_5	18	0.859	0.623	0.916	0.18	0.01	0.1

[a]Optimum number of factors.
[b]Mean of differences for duplicates.
[c]RMSE is the root mean square error = $\sqrt{(\Sigma(x_i - p_i)^2/n)}$, for n predictions p_i of a measured quantity x_i; $n = 16$. For duplicates, p_i is the mean of two predictions.
[d]Limits defined by least accurate determinations for independent test set (see also Figures 10 to 12).
[e]Excludes outliers A and B (see text and Figure 10a).

with respect to the calibration matrices (that is, extrapolation outside the composition range of the calibration data set). Thus, cement SRM 635 has an exceptionally high SO_3 content, almost twice as high as the highest value in C_c. In this case, the determination of clinker phases, calcium hydroxide, and calcium carbonate are accurate, but those of the sulfates and MgO show inaccuracies attributable to the extrapolation.

In contrast, SRM 1881 is not affected by extrapolation: its unusually low C_3S:C_2S ratio (also outside the range of C_c) is accurately predicted. Cements that have unusual composition can easily be added to the calibration data set in order to extend the reliable range of the model.

Extensions

Besides simple extensions of models such as M1 and M2 to increase the numerical range of the composition

TABLE 3. Quantitative analyses of standard reference cements by DRIFTS

	SRM 635		SRM 636		SRM 637		SRM 1881	
	Measured	Predicted	Measured	Predicted	Measured	Predicted	Measured	Predicted
C_3S	37	40	53	53	62	59	24	28
C_2S	25	31	26	26	20	19	46	44
C_3A	12	9	5	6	6	8	3	4
C_4AF	8	9	5	3	6	4	14	11
Gypsum	8.7	4.7	0.7	2.0	1.5	2.0	4.0	4.1
Bassanite	5.4	5.6	3.6	3.6	3.0	3.3	2.3	2.6
Syngenite	0.0	1.0	0.0	0.0	0.0	0.0	1.1	0.8
$Ca(OH)_2$	0.6	0.7	0.0	0.5	1.6	1.5	0.1	0.9
$CaCO_3$	1.00	1.00	0.50	0.30	0.04	0.30	0.08	0.0
$C_3S + C_2S$	62	69	79	80	82	77	70	72
SO_3	7.1	5.1	3.1	2.8	2.4	2.6	2.6	3.8
Na_2O	0.07	0.30	0.11	0.17	0.15	0.03	0.04	0.0
K_2O	0.45	0.90	0.59	0.36	0.25	0.10	1.20	1.00
MgO	1.20	2.50	2.60	2.30	0.67	1.29	2.60	2.90
P_2O_5	0.20	0.03	0.08	0.17	0.24	0.21	0.09	0.0

All data in wt %. Measured API clinker phase compositions are those calculated using certified oxides data. Predicted values are means of duplicate determinations.

matrix, calibration models can, of course, also be constructed to include new components. Many cements today are distributed as blends with admixtures of mineral fillers and pozzolans. We report elsewhere [36] that cements containing components such as hematite, silica flour, and barite can be rapidly and quantitatively analyzed by DRIFTS methods.

Concluding Discussion

The results presented show that the DRIFT spectrum provides a subtle and informative signature of a cement, in which is encoded information on its elemental and mineralogical composition. We have shown elsewhere [1] that particle-size information is also embodied in the DRIFT spectrum. In a qualitative sense, the spectrum of an unknown cement provides a rapid diagnostic tool which gives information on the nature and condition of the sample (A/F, sulfate mineralogy, aging, carbonation, etc.). In a quantitative mode, we demonstrate that high quality DRIFT spectra can be used with carefully constructed multivariate calibration models to provide some 14 items of compositional data with an accuracy that is adequate for many purposes. There is no doubt that models of this kind are capable of further refinement by extension of the calibration data set. The accuracy of predictions depends largely on the effort available to characterize the calibration materials. Here we have relied heavily on chemical analytical data, which has the virtue of high accuracy. On the other hand, direct mineralogical data on the clinker phases were lacking.

The quality of the results that can be achieved also very much depends on the quality of the practical procedures for sample preparation and spectroscopic analysis. However, round-robin studies involving blind tests with different spectrometers and different personnel have demonstrated levels of reproducibility similar to those that can be achieved in replicate tests by a single operator.

We have described the application of quantitative FTIR methods in the context of oilwell cementing. The most obvious application is to quality control in the field support laboratory. However, a rapid method of acquiring comprehensive mineralogical data is of value in the research and development laboratory. The nine-mineral/five-oxide representation of the composition presented here already provides a quite detailed view of compositional variation in cement materials. It goes some way beyond the Bogue representation in also giving estimates of the main minerals of the sulfate subsystem and of some of the products of aging. It therefore provides a rather direct way of monitoring the aging and deterioration of cements. There is no reason to believe that the particular FTIR spectrum → mineral transform presented here is optimal.

Acknowledgments

We acknowledge the essential contributions of many colleagues, especially those of Terry Bailey, Jean-François Baret, Peter Coveney, Vidhyadhar Gholkar, Geoffrey Maitland, Pierre Maroy, Michel Michaux, Eric Moulin, Erik Nelson, and Benoit Vidick.

References

1. Fletcher, P.; Coveney, P. *Adv. Cem. Bas. Mat.* **1995,** *2,* 21–29.
2. Hughes T.L.; Methven, C.M.; Jones, T.G.J.; Pelham, S.E.; Franklin, P. *5th International Symposium on Chemistry in the Oil Industry,* Ambleside, Cumbria, UK, April 1994; Royal Society of Chemistry: London (in press).
3. Hughes, T.L.; Jones, T.G.J.; Tomkins, P.; Gilmour, A.; Houwen, O.H.; Sanders, M. First International Conference on Health, Safety and Environment, 10–14 November 1991, The Hague, The Netherlands; SPE paper 23361.
4. Stark, P.B.; Herron, M.M.; Matteson, A. *Appl. Spect.* **1993,** *47,* 1820–1829.
5. Fredericks, P.M.; Doolan, K.J. *Mikrochim. Acta* **1988,** *11,* 127–132.
6. Uchikawa, H. *9th International Congress on the Chemistry of Cement,* Vol. 1; National Council for Cement and Building Materials: New Delhi, 1992; pp 794–883.
7. Simpson, B.E. *SPE Production Engineering* **1988,** 158–166.
8. *Rapid Methods for Chemical Analysis of Hydraulic Cement;* ASTM STP 985; Gebhardt, R.F., Ed. 1988.
9. Courtault, B.; Bellina, G.; Briand, G. *Analysis* **1987,** *15,* 227–236.
10. American Society for Testing and Materials. *Standard Test Methods for Chemical Analysis of Hydraulic Cement,* C 114–88.
11. Taylor, J.C.; Aldridge, L.P. *Powder Diffract.* **1993,** *8,* 138–144.
12. Campbell, D.H. *Microscopical Examination and Interpretation of Portland Cement Clinker;* Construction Technology Laboratories: Skokie, IL, 1986.
13. Stutzman, P.S.; Lenker, H.; Kanare, F.; Tang, F.; Campbell, D.H.; Struble, L. *11th International Conference on Cement Microscopy,* 10–13 April 1989, New Orleans, LA; International Cement Microscopy Association; Duncansville, TX, 1989; pp 154–168.
14. Lewis, G. In *Proceedings of the 2nd Symposium on Process Mineralogy;* Hagni, R.D., Ed.; AIME: Warrendale, PA, 1982; pp 271–285.
15. Bensted, J. *Cemento* **1980,** *77,* 169–182, 237–244.
16. Bensted, J.; Varma, S.P. *Cem. Technol.* **1974,** *5,* 378–382, 440–450.
17. Bensted, J. *Cemento* **1987,** *84,* 35–46.
18. Ghosh, S.N.; Handoo, S.K. *Cem. Concr. Res.* **1980,** *10,* 771–782.
19. Handoo, S.K.; Ghosh, S.N. *Prog. Cem. Concr.* **1992,** *1,* 222–252.
20. Bensted, J. *Cemento* **1990,** *87,* 137–146.
21. Bensted, J. *Cemento* **1976,** *73,* 45–51.
22. Bensted, J. *Naturwissenschaften* **1976,** *63,* 193.
23. Bell, G.M.M.; Bensted, J.; Glasser, F.P.; Lachowski, E.E.; Roberts, D.R.; Rodger, S.A. *Adv. Cem. Res.* **1993,** *5,* 71–79.

24. Henning, O. In *Infrared Spectra of Minerals;* Farmer, V.C., Ed.; Mineralogical Society: London, 1974.
25. American Petroleum Institute. *Specification 10A,* 21st ed.; API: Washington, 1991.
26. Fuller, M.P.; Griffiths, P.R. *Am. Lab.* **1978,** *10,* 69.
27. Fuller, M.P.; Griffiths, P.R. *Anal. Chem.* **1978,** *50,* 1906.
28. Kortüm, G. *Reflectance Spectroscopy;* Springer: New York, 1969.
29. Griffiths, P.R.; Fuller, M.P. *Adv. Infrared Raman Spectr.* **1982,** *9,* 63–129.
30. Krivacsy, Z.; Hlavay, J. *Spectrochim. Acta* **1994,** *50A,* 49–55.
31. Sharaf, M.A.; Illman, D.L.; Kowalski, B.R. *Chemometrics;* Wiley: New York, 1986.
32. Martens, H.; Naes, T. *Multivariate Calibration;* Wiley: Chichester, 1989.
33. Beebe, K.R.; Kowalski, B.R. *Anal. Chem.* **1987,** *59,* 1007A–1017A.
34. Taylor, H.F.W. *Adv. Cem. Res.* **1989,** *2,* 73–77.
35. Geladi, P.; MacDougall, D.; Martens, H. *Appl. Spectr.* **1985,** *39,* 491–500.
36. Hughes, T.L.; Methven, C.M.; Jones, T.G.J.; Pelham, S.E.; Vidick, B.; Fletcher, P. *Offshore Technology Conference,* 2–5 May 1994, Houston, TX; OTC paper 7582.